Full parameter extraction of a temperature-insensitive quantum well DFB laser using an optical injection technique

S. Ding, N. Doggett, D. Herrera, H. Huang, V. Kovanis, et al.

S. Ding, N. Doggett, D. J. Herrera, H. Huang, V. Kovanis, L. F. Lester, F. Grillot, "Full parameter extraction of a temperature-insensitive quantum well DFB laser using an optical injection technique," Proc. SPIE 12415, Physics and Simulation of Optoelectronic Devices XXXI, 124150D (10 March 2023); doi: 10.1117/12.2650460

SPIE.

Event: SPIE OPTO, 2023, San Francisco, California, United States

Full parameter extraction of a temperature-insensitive quantum well DFB laser using an optical injection technique

S. Ding[a,*], N. Doggett[b], D. J. Herrera[b], H. Huang[a], V. Kovanis[b], L. F. Lester[b], and F. Grillot[a,c]

[a]LTCI, Institut Polytechnique de Paris, Télécom Paris, 19 place Marguerite Perey, 91120, Palaiseau, France
[b]Bradley Department of Electrical and Computer Engineering, Virginia Polytechnic Institute & State University, Blacksburg, VA, 24061, USA
[c]Center for High Technology Materials, University of New-Mexico, Albuquerque, NM, USA

ABSTRACT

Distributed feedback lasers are key ingredients of high-speed, high-capacity integrated photonic chips. In this work, we extract the linewidth enhancement factor above threshold by measuring the transitional points in the optical-injection stability map from a quantum well distributed feedback laser with a temperature-controlled mismatch between the lasing and optical gain peaks. This unique measurement technique allows the simultaneous extraction of important parameters influencing the linewidth, particularly the photon lifetime. When the current is higher than twice threshold and 50 ℃, the linewidth enhancement factor is smaller than that at 10 ℃. This effect is attributed to the increasing differential gain at the lasing peak position, which is a result of the larger optical mismatch. We also measured the spectral linewidth at different temperatures, which then yields the spontaneous emission factor, n_{sp}. Due to the low linewidth enhancement factor at high temperatures, a large photon lifetime, and a modest increase in n_{sp}, the linewidth does not drastically increase with pump current and stays below 100 kHz at 50 ℃. Overall, the stability of the linewidth enhancement factor combined with the large optical mismatch brings a relative temperature insensitivity, which is of paramount importance for applications requiring high-temperature operation and improved coherent light.

Keywords: distributed feedback laser, optical injection, linewidth enhancement factor

1. INTRODUCTION

High stability and narrow linewidth lasers have diverse applications in gravitational wave detection, atomic clock, LiDAR, optical sensor and coherent communications.[1–4] Narrow linewidth lasers can boost scan rates, increase detection distances, and imaging clarity. For coherent communication and sensing, there is much effort towards developing narrow linewidth semiconductor lasers, beyond what is achievable with single Fabry-Perot or distributed feedback (DFB) resonators. To reduce the spectral linewidth, many approaches can be considered, including external cavity, phase-shifted and chirped grating, discrete mode DFB lasers, and fiber lasers. From the active region aspect, quantum dot (QD) DFB lasers, operating with very low population inversion can also produce spectral linewidth down to several kHz. Recently, much progress is reported on modal engineering of a DFB laser, in which light is generated in the III-V material and stored into the low-loss silicon material. This class of hybrid or heterogeneous integrated lasers indicates a promising path forward, where wavelengths down to 1 kHz level have already been demonstrated. Silicon photonic external cavity, Si_3N_4 ring resonators III-V/Si_3N_4 hybrid external cavity and other external cavity processes allow the linewidth of semiconductor lasers to be suppressed to several kHz.[5–7] On the other hand, the design of micro-ring resonator can also enhance the quality factor of the cavity, increase photon lifetime, achieve noise suppression and linewidth narrowing. The researchers used a CMOS process to cast the micro-ring resonator to obtain an ultra-high quality factor of 260 million, enabling semiconductor lasers with linewidth into Hz.[8] These approaches to obtain narrow linewidth lasers are very complicated nano-processes.

*shihao.ding@telecom-paris.fr

Physics and Simulation of Optoelectronic Devices XXXI, edited by Bernd Witzigmann, Marek Osiński, Yasuhiko Arakawa, Proc. of SPIE Vol. 12415, 124150D
 · 0277-786X · doi: 10.1117/12.2650460

Investigating the spectral linewidth also requires a systematic investigation on the relevant parameters of DFB lasers. Usually we extract the linewidth enhancement factor (α_H-factor) of the laser to evaluate the performance of linewidth and other dynamics properties.[9,10] The α_H-factor can be extracted by several methods. Below threshold, the amplified spontaneous emission (ASE) is commonly used to extract the α_H-factor. It relies on measuring the net modal gain change and tracking the wavelength drift at different sub-threshold bias currents.[11] To obtain the α_H-factor above the threshold, other measurement methods, such as optical injection or optical phase modulation can be considered.[12,13] Therefore, the above-threshold α_H of a single mode laser can be extracted from the optical injection-locking boundaries whereas the optical phase modulation can provide a comprehensive analysis of the α_H-factor across the the entire optical spectrum of a multimodes laser. But, it is important to stress that these two methods cannot release any other additional information about the DFB laser. In this paper, we consider a unique measurement technique focusing on the determination of the transitional points in the optical-injection stability map.[14] We show that this measurement technique constitutes an indirect method to extract the carrier-to-photon lifetime ratio as well as important parameters influencing the spectral linewidth of the DFB laser, particularly the α_H and the photon lifetime.

2. EXPERIMENTAL RESULTS AND DISCUSSION

Figure 1(a) depicts the optical power with current at the temperature ranging from 10 ℃ to 50 ℃. The QW DFB laser exhibits a superior stability at high temperatures. The threshold current varies slightly with temperature, being only 13.6 mA at 50 ℃. Owing to the high reflectivity coating design of both facets, the reduction in mirror loss decreases the threshold gain requirement, resulting in a very low threshold current (I_{th}). The current-dependent optical spectrum at different temperatures is shown in Figure 1(b), (c), and (d). The emission peaks move in the range between 1548 nm and 1552 nm as the temperature increases. The laser keeps an excellent spectral shape as the current increases over a temperature range of 10 ℃ to 50 ℃.

From the the ordinary differential equation (ODE) model of the optically-injected semiconductor laser, it has been shown that the α_H-factor can be directly extracted from the expression below:[14]

$$\frac{\Delta f_c/f_r}{\eta_{FH}/\eta_{RH}} = \frac{1}{2\sqrt{2}}\sqrt{(1+1/\alpha_H^2)(\alpha_H^2-1)^3} \tag{1}$$

where f_r is the free-running relaxation frequency. Δf_c is the measured critical detuning, which is located between Stable Locking, Period 1, and Four-Wave-Mixing (FWM), which is also called the Hopf-Saddle-Node point. When applied with zero detuning, η_{FH} and η_{RH} are the optical injection level at forward and reverse

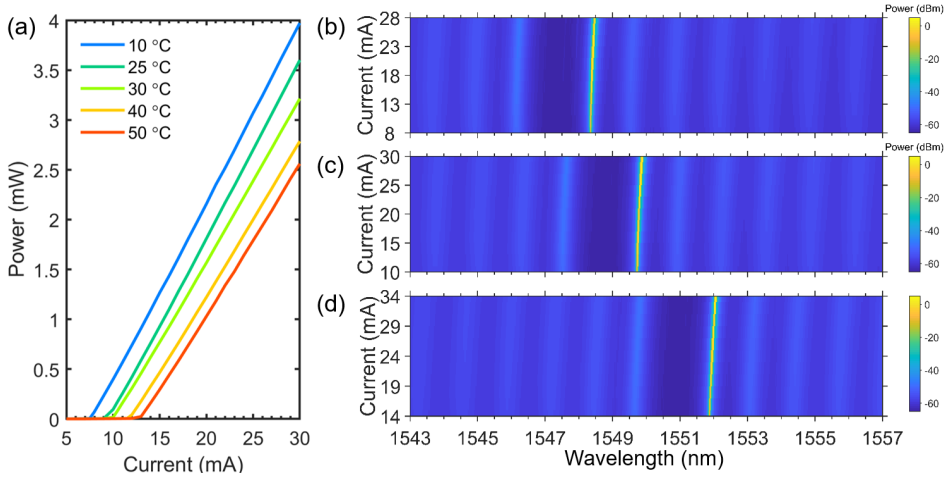

Figure 1. (a) Power-current characteristics measured at different temperature. Current dependent optical spectra measured at (b) 10 ℃, (c) 25 ℃, and (d) 50 ℃.

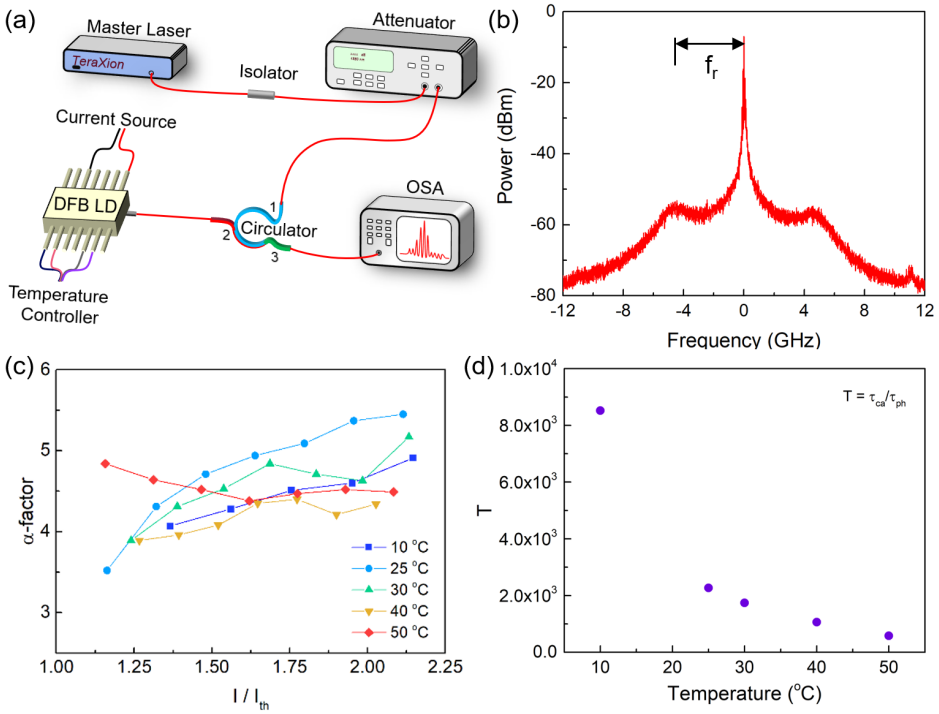

Figure 2. (a) Tabletop optical injection-locking experiment used for the α-factor extraction, (b) High resolution optical spectrum at 1.5 $\times$ I_{th} and 50 ℃, (c) Current-dependent α_H-factor at different temperature, and (d) Extracted T-value with the temperature.

Hopf bifurcation points respectively. When performing experiments, it is necessary to know the path loss from the master laser to the slave laser in order to calculate an accurate ratio of η_{FH}/η_{RH}. On the other hand, in (1) the α_H-factor which relates small variations of the real and imaginary parts of the refractive index due to a change of the carrier concentration, as the following expression:[15,16]

$$\alpha_H = -\frac{4\pi}{\lambda}\frac{\delta n/\delta N}{\delta G/\delta N} \tag{2}$$

where n is the carrier-induced refractive index, G is the gain, N is the carrier density, λ is the optical wavelength.

Figure 2(a) presents the tabletop optical injection-locking experiment used for the α_H-factor extraction. Here, a tunable laser is used as a master laser. Afterwards, an optical attenuator is set up to control the injection strength. The injected light then passes through the circulator to the slave laser. Finally, the light signal affected by the optical injection is received by a high-resolution optical spectrum analyser. When performing the experiment, first it is necessary to record the spectrum at a given current without injection, then extract the relaxation oscillation frequency and the position of the central peak. The optical spectrum at 1.5 I_{th} and 50 ℃is shown in Figure 2(b), which has a f_r of 4.5 GHz. Based on the position of free-running central peak, two Hopf bifurcation points can be derived by sweeping the injection strengthen under zero detuning. The central peak is also used to find the point under the Δf_c detuning, which is the intersection of the three dynamics. The pump dependent α_H-factor at different temperatures is demonstrated in Figure 2(c) using this approach. It shows that the α_H-factor increases with the bias current which is expected as a result of the gain compression. The evolution with temperature does not have a clear trend. Such a variation with temperature requires more investigation since it is mostly determined mainly by the change of the effective index due to the change of the crystal lattice temperature, and not only by the carrier plasma temperature. The ratio of the spontaneous carrier lifetime τ_{ca} to the photon lifetime τ_{ph} is defined as the T parameter and can be estimated from the injection locked system.[14] It is significant that T decreases exponentially with increasing temperature as shown in Figure 2(d). Indeed,

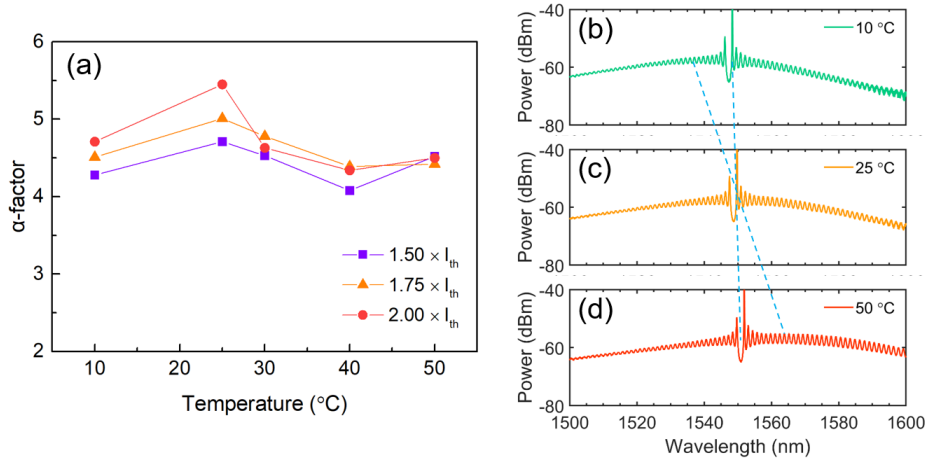

Figure 3. (a) Temperature dependent α_H-factor measured at different pump current. Free-running optical spectrum at (b) 10 ℃, (c) 25 ℃, (d) 50 ℃and $1.5 \times I_{th}$.

as the temperature increases, the carriers are more quickly involved in the nonradiative recombination, hence resulting in a reduced carrier lifetime.[17,18] At room temperature, the T is found to be about 2,000 which is a typical value for a semiconductor laser with interband transitions. Here, we show that the optical injection locking technique constitutes a unique tool to extract the T parameter and to qualitatively analyze the variation of carrier recombination mode in semiconductor lasers.

In order to explore the trend of α_H-factor with temperature and current in detail, the plot of the α_H with temperature for different pump current is shown in Figure 3(a). When the temperature is below than 30 ℃, the α_H-factor increases with the pump current, but the variation of α_H-factor is less than 1. No significant increase in the α_H with current occurs at above 30 ℃which confirms its strong temperature stability. In order to better understand this behavior, optical spectra were extracted at 1.5 times the threshold current and at 10 ℃, 25 ℃, and 50 ℃, as shown in Figure 3(b,c,d). The gain peak is located to the left of the DFB lasing peak at 10 ℃. As the temperature increases, both the gain peak and the DFB lasing peak are red-shifted. However, the gain peak moves more rapidly, causing the DFB lasing peak to move to the right of the gain peak at higher temperatures. As shown in,[19] there exists a critical temperature (T_c) for which the gain peak and the DFB lasing peak are in the same position, thus providing a smaller α_H-factor and a maximum differential gain. In this DFB laser, the T_c is estimated to be around 25 ℃. The optical mismatch between the gain peak and the DFB lasing peak effectively increases the temperature tolerance of the α_H because of its spectral dependence, therefore the relative leftward shift of the DFB lasing peak can facilitate the reduction of the α_H-factor.[19,20] At 50 ℃, although the DFB lasing peak moves to the left of the gain peak, the differential gain is reduced at this point, which makes the α_H not always decreasing anymore. In addition, more non-radiative recombinations are introduced at high temperature based on the change in the T value (Figure 2(d)), which can also affect the α_H-factor. As a result, a portion of the carriers do not contribute to the variation of the gain, causing the denominator term ($\delta G/\delta N$) to become smaller, and making the α_H-factor larger. Therefore, the positive effect of the optical mismatch combined with the negative one from the non-radiative recombination at high temperature can explain the complex variations of the α_H-factor.

In this last section, we want to investigate the impact the α_H-factor, in particular its remarkable temperature stability, has on the spectral linewidth. To do so, we used the delayed self-heterodyne interferometric method to gauge the linewidth as shown in Figure 4(a). The laser beam has to pass through two isolators to prevent back-reflections in the system affecting the linewidth. Then, the split beams are routed into an acousto-optic modulator (AOM) with 100 MHz beatnote and a 25 km fibre coil respectively. Finally, the combined light arrives at the photodetector (PD) to produce the signal that enters the electrical spectrum analyser (ESA) to obtain a linewidth spectrum. Figure 4(b) presents the pump dependent linewidth at 10 ℃, 25 ℃, and 50 ℃, respectively. All linewidths were extracted by using a Voigt fitting. At 10 ℃, the linewidths above the threshold current are

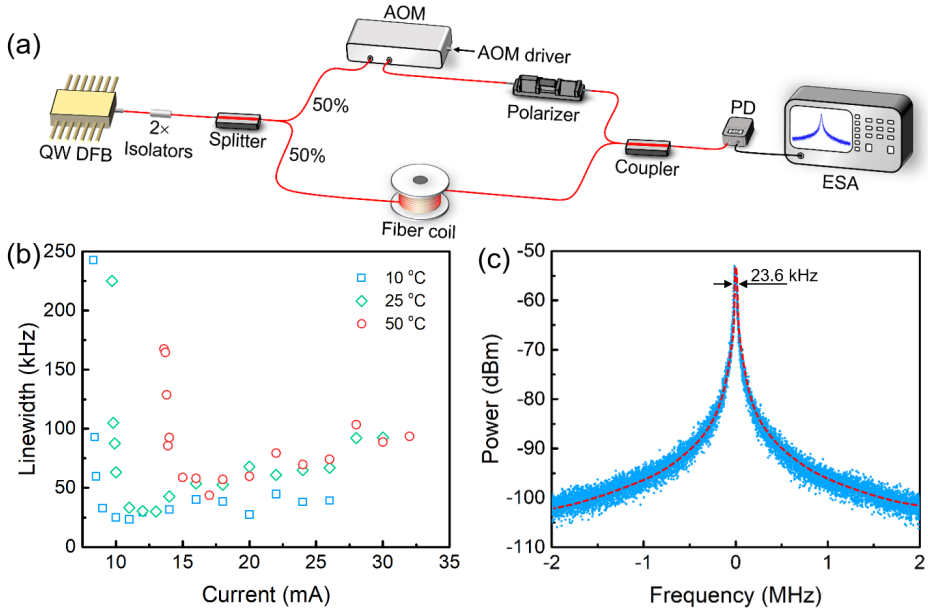

Figure 4. (a) Set-up of delayed self-heterodyne interferometric method for extracting the spectral linewidth. (b) Pump dependent linewidth at 10 ℃, 25 ℃, and 50 ℃. (c) RF spectrum and the corresponding Voigt fitted curve.

all less than 50 kHz and flatten out as the current increases. The Voigt fitting of the beatnote in Figure 4(c) leads a minimum linewidth of 23.6 kHz. At 25 ℃, and 50 ℃, the injected current affects the linewidth, since a rebroadening is observed. In fact, the linewidth rebroadening is known to occur in any semiconductor laser due to thermal effects, mode instability, longitudinal spatial hole burning, and gain compression. Despite that, the results show that the minimum linewidth remains very small at 30.4 kHz and 43.7 kHz respectively. Even at twice the threshold current, the linewidth remains less than 100 kHz which is very narrow for a free-running QW DFB laser made without any artificial solutions. Here, the narrow linewidth is achieved thanks to the long photon lifetime which is obtained from the high power reflectivity on both facets. In addition, the large optical mismatch implemented in this DFB structure leads to a stable variation of the α_H with the injection current especially at high temperature. The interplay between these two parameters makes the spectral linewidth narrow and constrained within the temperature range.

3. CONCLUSION

In this work, a QW DFB laser without an external cavity was extracted with full parameters by optical injection locking technique. In particular, the α_H-factor and the ratio of carrier lifetime to photon lifetime, which are the parameters intimately associated with linewidth. The high temperature tolerance of the α_H-factor caused by the optical mismatch allows the linewidth to exhibit a strong temperature stability. And the high reflectivity cavity facets design drives the QW DFB laser with a record linewidth down to 23.6 kHz at 10 ℃. Overall, this work also provides further ideas such as using quantum dot lasers for linewidth reduction, which is of paramount importance for applications requiring high-temperature operation and improved coherent light.

REFERENCES

[1] Abramovici, A., Althouse, W. E., Drever, R. W., Gürsel, Y., Kawamura, S., Raab, F. J., Shoemaker, D., Sievers, L., Spero, R. E., Thorne, K. S., et al., "Ligo: The laser interferometer gravitational-wave observatory," *science* **256**(5055), 325–333 (1992).

[2] Bloom, B., Nicholson, T., Williams, J., Campbell, S., Bishof, M., Zhang, X., Zhang, W., Bromley, S., and Ye, J., "An optical lattice clock with accuracy and stability at the 10- 18 level," *Nature* **506**(7486), 71–75 (2014).

[3] Wu, Y., Deng, L., Yang, K., and Liang, W., "Narrow linewidth external cavity laser capable of high repetition frequency tuning for fmcw lidar," *IEEE Photonics Technology Letters* **34**(21), 1123–1126 (2022).

[4] Guan, H., Novack, A., Galfsky, T., Ma, Y., Fathololoumi, S., Horth, A., Huynh, T. N., Roman, J., Shi, R., Caverley, M., et al., "Widely-tunable, narrow-linewidth iii-v/silicon hybrid external-cavity laser for coherent communication," *Optics express* **26**(7), 7920–7933 (2018).

[5] Kobayashi, N., Sato, K., Namiwaka, M., Yamamoto, K., Watanabe, S., Kita, T., Yamada, H., and Yamazaki, H., "Silicon photonic hybrid ring-filter external cavity wavelength tunable lasers," *Journal of Lightwave Technology* **33**(6), 1241–1246 (2015).

[6] Stern, B., Ji, X., Dutt, A., and Lipson, M., "Compact narrow-linewidth integrated laser based on a low-loss silicon nitride ring resonator," *Optics letters* **42**(21), 4541–4544 (2017).

[7] Zhu, Y. and Zhu, L., "Narrow-linewidth, tunable external cavity dual-band diode lasers through inp/gaas-si 3 n 4 hybrid integration," *Optics express* **27**(3), 2354–2362 (2019).

[8] Jin, W., Yang, Q.-F., Chang, L., Shen, B., Wang, H., Leal, M. A., Wu, L., Gao, M., Feshali, A., Paniccia, M., et al., "Hertz-linewidth semiconductor lasers using cmos-ready ultra-high-q microresonators," *Nature Photonics* **15**(5), 346–353 (2021).

[9] Köster, F., Duan, J., Dong, B., Huang, H., Grillot, F., and Lüdge, K., "Temperature dependent linewidth rebroadening in quantum dot semiconductor lasers," *Journal of Physics D: Applied Physics* **53**(23), 235106 (2020).

[10] Duan, J., Huang, H., Lu, Z., Poole, P., Wang, C., and Grillot, F., "Narrow spectral linewidth in inas/inp quantum dot distributed feedback lasers," *Applied Physics Letters* **112**(12), 121102 (2018).

[11] Duan, J. N., Huang, H. M., Dong, B. Z., Norman, J. C., Zhang, Z. Y., Bowers, J. E., and Grillot, F., "Dynamic and nonlinear properties of epitaxial quantum dot lasers on silicon for isolator-free integration," *Photonics Research* **7**(11), 1222–1228 (2019).

[12] Liu, G., Jin, X., and Chuang, S.-L., "Measurement of linewidth enhancement factor of semiconductor lasers using an injection-locking technique," *IEEE photonics Technology letters* **13**(5), 430–432 (2001).

[13] Ding, S., Dong, B., Huang, H., Bowers, J., and Grillot, F., "Spectral dispersion of the linewidth enhancement factor and four wave mixing conversion efficiency of an inas/gaas multimode quantum dot laser," *Applied Physics Letters* **120**(8), 081105 (2022).

[14] Herrera, D. J., Kovanis, V., and Lester, L. F., "Using transitional points in the optical injection locking behavior of a semiconductor laser to extract its dimensionless operating parameters," *IEEE Journal of Selected Topics in Quantum Electronics* **28**(1), 1–9 (2021).

[15] Henry, C., "Theory of the linewidth of semiconductor lasers," *IEEE Journal of Quantum Electronics* **18**(2), 259–264 (1982).

[16] Duan, J., Huang, H., Jung, D., Zhang, Z., Norman, J., Bowers, J., and Grillot, F., "Semiconductor quantum dot lasers epitaxially grown on silicon with low linewidth enhancement factor," *Applied Physics Letters* **112**(25), 251111 (2018).

[17] Hild, K., Marko, I. P., Johnson, S. R., Yu, S.-Q., Zhang, Y.-H., and Sweeney, S. J., "Influence of de-tuning and non-radiative recombination on the temperature dependence of 1.3 μ m gaassb/gaas vertical cavity surface emitting lasers," *Applied Physics Letters* **99**(7), 071110 (2011).

[18] Sweeney, S., McConville, D., Masse, N., Bouyssou, R.-X., Adams, A., Ahmad, C., and Hanke, C., "Temperature and pressure dependence of recombination processes in 1.5 μm ingaalas/inp-based quantum well lasers," *physica status solidi (b)* **241**(14), 3391–3398 (2004).

[19] Dong, B., Duan, J., Huang, H., Norman, J. C., Nishi, K., Takemasa, K., Sugawara, M., Bowers, J. E., and Grillot, F., "Dynamic performance and reflection sensitivity of quantum dot distributed feedback lasers with large optical mismatch," *Photonics Research* **9**(8), 1550–1558 (2021).

[20] Yamanaka, T., Yoshikuni, Y., Yokoyama, K., Lui, W., and Seki, S., "Theoretical study on enhanced differential gain and extremely reduced linewidth enhancement factor in quantum-well lasers," *IEEE journal of quantum electronics* **29**(6), 1609–1616 (1993).